

Solutions Mixing Visualization in Continuous-Flow Microreactors via Interferometric Technique

E.A. Mosheva^{1,A,B}, A.V. Shmyrov^{2,A,B}, A.I. Mizev^{3,A,B}

^A Institute of Continuous Media Mechanics RAS, Perm, Russia

^B Perm National Research Polytechnic University, Perm, Russia

¹ ORCID: 0000-0002-5722-2814, mosheva@icmm.ru

² ORCID: 0000-0003-0683-7971, shmyrov@icmm.ru

³ ORCID: 0000-0001-5233-8271, alex_mizev@icmm.ru

Abstract

The paper demonstrates the potential of interferometry as a visualization technique for studying the mixing processes of liquid reagents in continuous-flow microreactors. We visualized two types of instabilities: double-diffusion convection and Marangoni soluto-capillary convection. We employed two optical schemes, depending on how large values of refractive index inhomogeneities resulting from instabilities needed to be visualized, including the shear interferometer and the Fizeau interferometer. The interferometry enabled a qualitative investigation of the structure and dynamics of the generated convection. In addition, by implementing the phase shift method by the IntelliWave program, we quantified the efficiency of the mixing process between pumped liquids. These quantitative findings complemented our qualitative visualization, providing further evidence of the effectiveness of interferometry in studying mixing processes. Our results confirm that the interferometry technique is an effective tool for the visualization and analysis of convective flows in continuous-flow microreactors. Moreover, the insights gained from this research contribute to the broader understanding and optimization of mixing processes in microreactor systems.

Keywords: microchannel, Marangoni convection, concentration-capillary convection, interface, shear interferometry, Fizeau interferometry.

1. Introduction

Continuous-flow microreactors are innovative systems extensively utilized in various scientific and industrial fields. These systems are designed to conduct chemical reactions by continuously transporting reagents through specialized microchannels. This approach offers numerous advantages compared to traditional batch reactors and has gained widespread adoption in pharmaceuticals, organic synthesis, and other industries. Continuous-flow microreactors make the technological process not only continuous but also highly productive. The constant input of reagents and removal of reaction products result in heightened efficiency and resource conservation. Furthermore, these microreactors enable precise control of reaction conditions through the reagent flow regulation and flexible temperature management. In addition, their compact size allows for improved scalability and economic efficiency [1, 2].

However, continuous-flow microreactors also present certain drawbacks. Firstly, their small channel size predominantly results in laminar flow, which restricts efficient mixing and makes the distribution of velocity and concentration non-uniformly. This limitation hampers the potential use of flow microchannels, especially in applications requiring a high level of flow uniformity. Mutual diffusion of reagents in the transverse direction is the primary mechanism of mass transfer, necessitating an increase in channel length to achieve complete mixing. Researchers have proposed various strategies to enhance liquid mixing in continuous-flow reactors [3-5]. One approach involves enhancing the flow mixing by modifying the inter-

nal topology of the reactor [6, 7]. Another method employs external force fields, such as ultrasonic waves or electromagnetic fields, to induce mass transfer within the channel [5, 8]. We previously demonstrated that gravitational field can also serve the same purpose by creating specific conditions that trigger hydrodynamic instabilities. Notably, we illustrated that by exploiting the disparities in density or diffusion coefficients of the pumped reagents, it is possible to promote reagent mixing through gravity-dependent instability mechanisms [9]. The second challenge with microreactors is their small size, which complicates and sometimes restricts the use of visualization and measurement techniques for studying mass transfer processes. Currently, various visualization methods are commonly employed. These include fluorescent markers that allow visualization mixing and monitor flow characteristics, optical microscopy methods, and techniques that rely on indicator reactions for qualitative and quantitative assessment of mixing. The most accessible approach involves adding different dyes (such as fluorescent, pH-sensitive, and food-grade dyes). However, previous research has shown that dye addition can lead to erroneous results [10]. Dissolving a dye in the system is akin to adding a new component with its density, diffusion coefficients, and surface tension, which can quantitatively and even qualitatively change the nature of the mixing process.

Methods that visualize the refractive index field in solution offer advantages over other techniques. They include shadowgraph and interference methods. Shadowgraph techniques, such as synthetic schlieren [11], are straightforward to implement and require basic instrumentation. However, their main drawback is low sensitivity. In contrast, interference techniques [12] exhibit much higher sensitivity. Experimental implementation of interferometry is not significantly more complex but necessitates more expensive equipment. The sensitivity of interference methods in hydrodynamic problems relies on the dynamic range of the video camera used to record the interferogram. A conventional industrial 8-bit video camera with a dynamic range (DR) exceeding 50 dB enables the detection of optical path differences (OPD) as small as 1/100 of a wavelength. The utilization of scientific-grade cameras allows for achieving sensitivities of 1/1000 (DR > 70 dB) or even 1/10000 of the wavelength (in case of expensive 16-bit cameras with DR > 90 dB). Furthermore, employing multi-pass interferometric schemes, such as the Fabry-Perot type, can enhance the sensitivity of interferometry, providing almost unlimited potential. However, researchers commonly prefer using double-pass schemes such as Michelson or Fizeau types because they are easier to implement.

Interferometric technology has its drawbacks as well. Its high sensitivity prevents the registration of significant refractive index gradients beyond the resolution of the video camera. In simple continuous-flow reactors (with Y or T-junction), high refractive index gradients occur near the merging point of two incoming streams, where diffusion has not yet blurred the mixing zone. In such cases, a shear interferometer can be used [13]. The shear interferometer's optical scheme involves dividing the light beam into reference and object beams after passing through the studied inhomogeneity. As a result, the object wavefront interferes with its copy, shifted across the optical axis. By reducing the magnitude of the shift, we can decrease the interferometer sensitivity, enabling the resolution of significant refractive index inhomogeneities. The interference fringes on the interferogram correspond to the refractive index gradient, similar to the shadowgraph method. Therefore, this technique shares the same limitations as the shadowgraph method. To obtain quantitative information about the refractive index distribution, one can integrate a specific segment in the direction of the shift. The process of integration introduces an additional variable error into the final result. Note, that a complete reconstruction of the refractive index field requires a minimum of two interferograms obtained with a shift in two perpendicular directions unless the refractive index field exhibits axial or mirror symmetry (a common situation in hydrodynamics). Hence, the shear interferometer proves valuable for the qualitative analysis of convective structures characterized by significant refractive index gradients. However, in other cases, it is recommended to utilize interferometers assembled using a two-pass scheme that enables the visualization of flow structure and facilitates precise quantitative data acquisition regarding the refractive index field.

This article presents the visualization results obtained using a shear interferometer and a Fizeau autocollimation interferometer. Both schemes visualized the mixing process of two aqueous solutions within a continuous-flow reactor under conditions of hydrodynamic instability formation. We investigate two types of instability, gravity-dependent and gravity-independent. In the case of gravity-dependent instability, we use the shear interferometer to visualize the flow structure arising from the formation of double-diffusion convection [14]. In the case of gravity-independent instability, we used the Fizeau interferometer to visualize the development of Marangoni convection [15]. Additionally, the Fizeau interferometer allows for the acquisition of quantitative information regarding changes in the refractive index, facilitating an evaluation of the effectiveness of the micro-mixer operating based on the Marangoni effect.

2. Experimental setup

2.1. Microreactor

We performed experiments in a continuous-flow microreactor with a mixing zone in the form of a long rectilinear microchannel (Figure 1). The microreactor's side walls were constructed from transparent plane-parallel glass plates with a thickness of 2 mm. A chemically resistant spacer was positioned between the plates to define the location of the supply channels and the mixing zone. The microreactor's side walls have special holes. It allowed for the supply and withdrawal of liquids via tubes connected to a syringe pump. The design of the microreactor used offered flexibility in terms of adjustment, as changing the shape and geometric dimensions of the mixing zone only required replacing the spacer, thereby avoiding the complete reconstruction of the microreactor.

The first set of experiments focused on visualizing and investigating the mixing process of aqueous solutions induced by a gravity-dependent type of instability, namely double-diffusion convection (DD). This instability arises due to the difference in the molecular diffusion coefficients between the components dissolved in the system. In the case of initially stationary two-layer system formed by homogeneous solutions of two different substances, instability develops in the form of finger-like convective structures that symmetrically propagate in both directions from the initial contact zone of the liquids [14]. To study the effect of this type of convection on the mixing process, we used a Teflon spacer with a thickness of 1500 microns (Figure 1a). The contact of the initial solutions took place in the Y-junction located at the base of the microchannel. The lower arm of the Y-channel supplied a denser aqueous solution of faster diffusing potassium chloride (KCl) with a mass concentration of 11.3%. Simultaneously, the upper arm of the Y-channel delivered a less dense aqueous solution of slower diffusing copper (II) chloride (CuCl_2) with a mass concentration of 6.3%. The initially stable density stratification excluded the development of Rayleigh-Taylor instability. The presence of a faster diffusing solute in the lower layer was a prerequisite for the formation of double-diffusion convection [14].

In the second series of experiments, our objective was to study the impact of soluto-capillary Marangoni convection, a gravity-independent hydrodynamic instability, on the mixing process of initial solutions. This instability arises in the presence of a liquid-liquid or liquid-gas interface, along which a surface tension gradient is created due to a concentration gradient of surfactant located at the interface [15]. In these experiments, we utilized a silicone spacer with a thickness of 200 microns (Figure 1b). The contact of the initial solutions took place at the T-junction located at the base of the microchannel. In these experiments, the lower arm of the T-channel supplied the denser pure water. The upper arm of the T-channel delivered a less dense aqueous solution of isopropyl alcohol with a mass concentration of 9.6%. An additional inlet tube located at the upper boundary of the microchannel provided an air supply to create a gas bubble inside the microreactor. It formed a liquid-gas interface inside the microchannel, adjacent to the diffusion zone between the pumped solutions.

In both sets of experiments, the microchannel had a length of $L=7$ cm and a height of $h=0.2$ cm. The flow rate ranged from $Q = 0.001$ to 0.02 ml/min, corresponding to a flow velocity range of $v=0.033$ to 0.066 cm/s. When operating within this flow range, we tightly clamped the silicone spacer between the side glass plates to ensure leak-free conditions. This becomes possible because silicone has high adhesion to glass, unlike other materials, and securely "sticks" without the need for gluing. However, for the Teflon spacer, we sealed the perimeter of the microreactor with glue. All experiments were performed at an ambient temperature of 22 ± 1 °C.

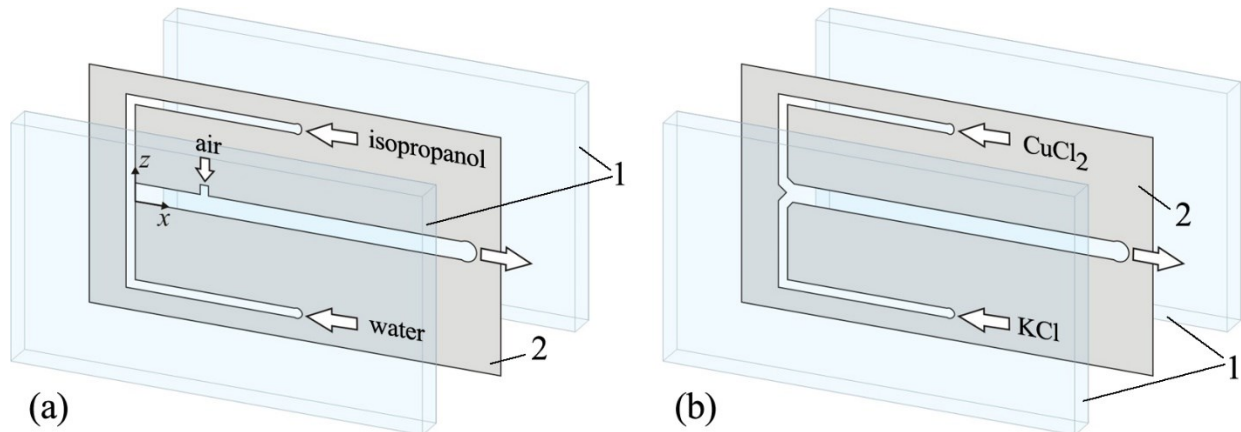


Figure 1. The diagram of the microreactor: 1 – side glass walls of the microreactor, 2 – the spacer defining the geometry of the microreactor. Large arrows indicate the position of the inlets and outlet channels. A small arrow demonstrates the air supply inlet used to create a liquid-gas interface inside the microreactor during the study of Marangoni convection.

2.2. Interferometry schemes

2.2.1. Visualization of large inhomogeneities (using the example of double-diffusion instability)

We used a laser interferometer to visualize the flow structure and study the mixing process. We applied two different optical schemes, depending on the type of hydrodynamic instability. In the first case, we investigated the development of double-diffusion convection. The instability occurs directly at the junction point of the flows. Convection induces significant concentration variations, leading to the formation of regions characterized by large refractive index gradients. To visualize these phenomena, we employed a shearing interferometer. Figure 2 depicts the optical scheme of the interferometer and an example of the flow structure visualization in the case of the development of the double-diffusion convection. Also, in Figure 2, for comparison, the visualization of the flow in the non-convective case, when mixing solutions in the transverse flow direction occurs solely due to diffusion, is given. In this optical scheme, two glass plane-parallel plates of interference quality 2, located parallel to one another at a small distance $d/\sqrt{2}$ (see Fig. 2), are used to split the wavefront passed through the inhomogeneity. The wavefront is incident on the plates at an angle of 45° and reflected mainly from the back plane of the first plate and front plane of the second plate, which have a semitransparent coating. As a result, two identical reflected wavefronts laterally sheared relative to each other by an amount of d are projected on the camera matrix 4. The d value is modified using a special adjustment screw that enables fine-tuning the wavefront shearing and, therefore, an interferometer sensitivity.

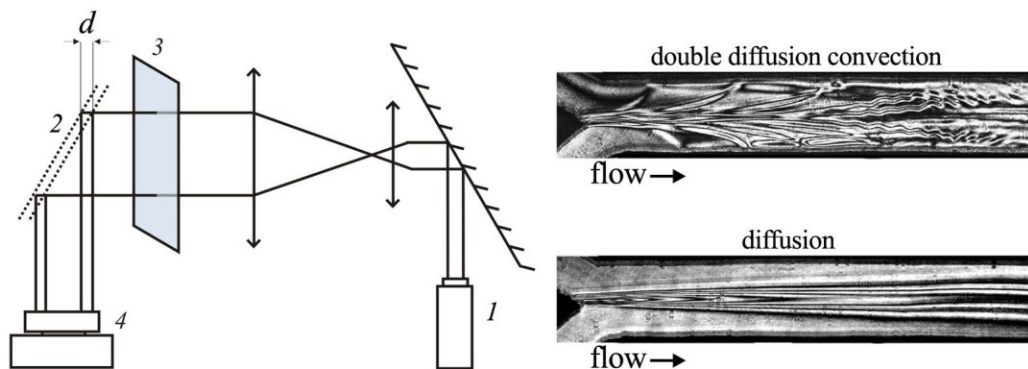


Figure 2. Scheme of the optical setup: 1 - He-Ne laser, 2 - the element responsible for implementing the shift, 3 - microreactor; 4 - CCD camera. The d value is 0.1 mm. The vertical size of each interferogram is 25 mm.

In contrast to a stationary liquid condition ($Q=0$ ml/min), where the instability leads to the symmetric spreading of a finger-like convective structure in both directions from the initial contact zone, the presence of liquid pumping ($Q>0$) significantly alters the flow structure. At the beginning of the channel, the original layers remain unmixed, and a thin diffusion mixing zone forms between them, characterized by a large concentration gradient. Moving away from the Y-junction, DD-convection gives rise to a convective structure around the diffusion zone. The continuous flow of liquids along the microchannel carries developing "fingers" from the point of their origin, causing them to elongate and leading to a more intricate structure (Fig. 2, top interferogram). An interferogram demonstrating the mixing of liquids in the absence of convection, solely reliant on diffusion, is provided for comparison in the same figure. A comparison of the interferograms highlights that the development of DD convection leads to flow splitting, folding, and recombination, similar to how it happens in microreactors with complex geometries. It is known [7] that such microreactors, utilizing internal partitions, obstacles, turns, and irregularities, transform the initial laminar flow into turbulence, facilitating more efficient mixing through the development of forced convection. In the present study, similar outcomes are achieved through the mechanism of natural convection, eliminating the need to use reactors with complex geometries.

2.2.2. Visualization of weak inhomogeneities (using the example of Marangoni convection)

In the second case, we examined the development of soluto-capillary Marangoni convection. Our study involved a two-layer system with stable density stratification, consisting of an aqueous solution of isopropyl alcohol and water. To trigger Marangoni convection, a gas bubble was formed near the top boundary of the microchannel at a distance of 1.1 cm from the T-junction, creating a liquid-gas interface. We visualized the spatial distribution of the solute using the Fizeau interferometer. Figure 3 depicts the optical scheme and provides examples of interferograms. The interference pattern was formed by a pair of plane-parallel glass plates of interference quality with semitransparent coating (2 and 4), which formed the Fizeau interferometer cell. The side walls of the microfluidic channel were positioned at a slight angle to the optical axis of the interferometer to prevent the reflected light from the reactor walls from entering the camera's aperture. While glass plate 2 remained fixed, the angle of plate 4 was adjustable. In position I, where the plates were precisely parallel to each other and perpendicular to the optical axis, the interferometer allowed us to observe patterns in the infinite fringe mode (see interferogram I in Figure 3). This optical configuration allowed the investigation of the emerging flow structure and provided a qualitative assessment of the mixing intensity of the liquids.

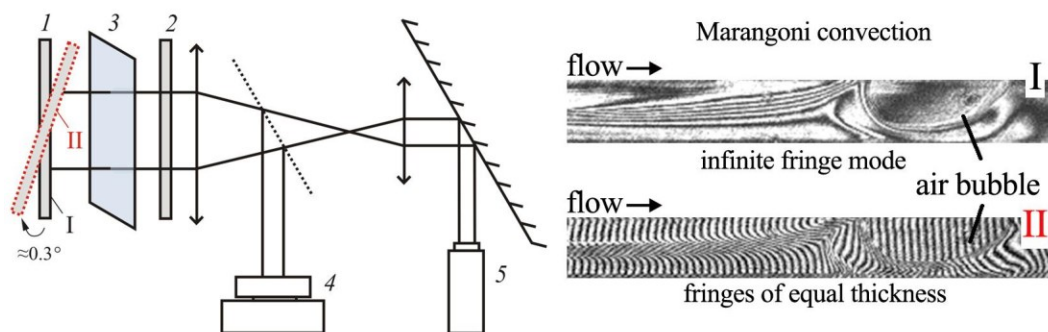


Figure 3. Scheme of the optical setup: 1, 2 – interference glass plates forming the measuring cell of the Fizeau interferometer; 3 - microreactor; 4 - CCD camera, 5 - He-Ne laser. The vertical size of each interferogram is 0.2 cm.

In order to observe the mixing process in the mode of fringes of equal thickness, the interferometer was readjusted using special screws (see Interferogram II in Figure 3). This adjustment involved introducing a slight angle ($\sim 0.3^\circ$) between the glass plates of the interferometer. Interferograms obtained in this manner were suitable for qualitative analysis and quantitative assessment of the refractive index distribution resulting from the non-uniform concentrations of the dissolved substance (specifically, alcohol in this study). For the quantitative analysis, we employed the spatial phase shift method [16]. We processed the interferograms and measured the quantitative parameters using the IntelliWave software (Mahr GmbH, Germany).

No specific requirements were imposed on the quality of the glass walls of the microreactor when implementing this optical scheme. It was sufficient for the utilized glasses to be visually free from any noticeable optical distortions, such as internal striae and surface deformations. The spacer, which defines the channel geometry, should possess a consistent and uniform thickness. This requirement is essential to minimize the measurement error of the refractive index difference of the liquid, ultimately enabling precise determination of the concentration gradient across different segments of the microreactor. For instance, the silicone spacer had a thickness of $200 \pm 5 \mu\text{m}$, resulting in a relative measurement error of $\pm 2.5\%$.

3. Image processing

3.1. Calculation of the Optical path difference field

The interferograms (fringes of equal thickness) enabled the reconstruction of two-dimensional optical path difference (OPD) fields using the phase shift method. Moreover, essential parameters of the study, such as the distribution of refractive index or the concentration of the dissolved substance, could also be calculated. The interferogram, obtained by reflecting light from the coatings on the interference glass plates, contained integral information about the optical path difference (OPD). This OPD consisted of information obtained from the light passing through the investigated liquid system (a signal), the microfluidic cell walls, and the air space between the interference plates and microchannel (a noise). To extract the OPD of the desired signal, we captured a reference image that contained only noise. This reference image was an interferogram obtained for a microchannel filled only with pure water. Subsequently, the IntelliWave software functions were employed to extract the OPD of the reference image to reconstruct the wrapped phase difference field and the corresponding OPD field. Figure 4a illustrates the interferogram of the water-filled microreactor and corresponding wrapped phase difference and OPD fields.

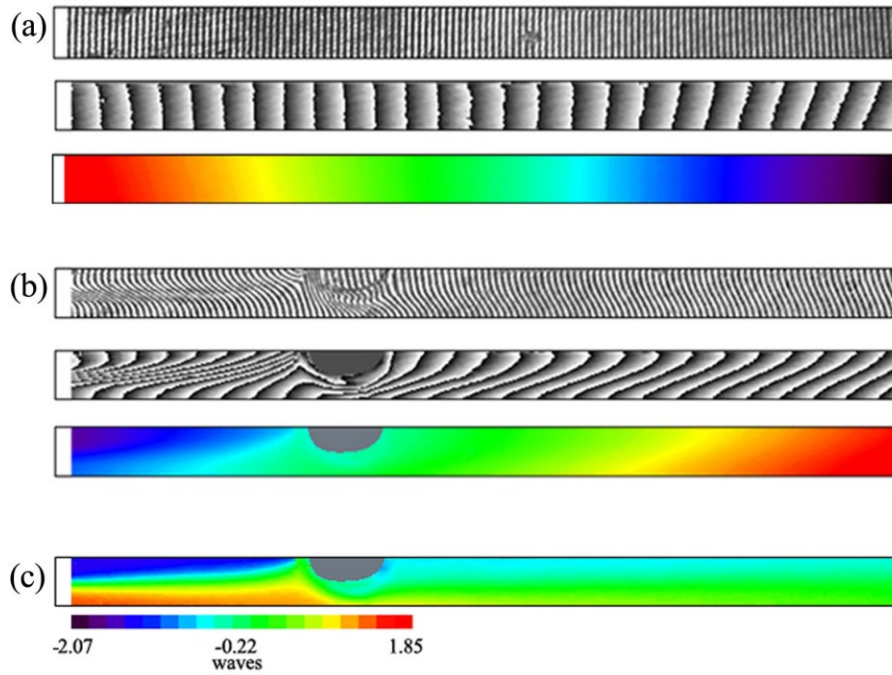


Figure 4. The main stages of image processing shown in the example of interferogram analysis obtained at $Q=0.004$ ml/min. From top to bottom: an interference pattern (fringes of equal thickness), the corresponding wrapped phase difference field, and the OPD field acquired in a microreactor filled with (a) water (reference image) and (b) the system alcohol-water. (c) The resulting OPD field, representing the alcohol concentration distribution obtained by subtracting the OPD of the reference image. The bubble position is $x=1.1$ cm. The working region of the channel is indicated by a black frame, aligned with the chosen coordinate axes shown in Figure 1a. Each image has a vertical size of 0.2 cm.

Once the OPD field of the reference image was obtained, we initiated the pumping of the working liquids and created a gas bubble inside the channel. In the presence of an interfacial boundary within the system, an additional mixing mechanism arises due to soluto-capillary Marangoni convection. Isopropyl alcohol acts as a surfactant and reduces the surface tension of the solution. As a result, a surface tension gradient forms along the free surface adjacent to the diffusion zone between water and alcohol. It initiates the development of intense capillary flow both at the interfacial surface and in the vicinity of the bubble. The resulting convection homogenizes the distribution of alcohol, leading to the disappearance of the surface tension gradient and the decay of convection. However, due to the continuous supply of working liquids, the initial concentration distribution near the free surface is reinstated, thereby reinitiating the Marangoni mechanism. Thus, the system enters an oscillatory regime of soluto-capillary Marangoni convection [12] that acts as a local micro-mixer that stirs the liquids near the bubble surface. An example interferogram demonstrating the process of liquid mixing under the development of Marangoni convection, along with its corresponding reconstructed wrapped phase difference and OPD fields (raw signal, without noise signal subtraction), are depicted in Figure 4b. The resulting OPD field, which demonstrates the refractive index changes of the mixed liquids within the channel, is presented in Figure 4c.

3.2. Calculation of the concentration difference

For any vertical cross-section of the two-dimensional OPD field, we can calculate the refractive index distribution $n(z)$. Then, using the concentration-dependent refractive index dependence $n(C)$ for each vertical cross-section, concentration profiles $C(z)$ can be obtained, which further allows calculating the concentration difference ΔC in the cross-section. This parameter served as a criterion for assessing the efficiency of mixing. By analyzing how the initial concentration difference ΔC between layers changes along the channel, we quantitatively

evaluated the mixing efficiency in the presence of Marangoni convection. Figure 5 presents the results obtained from experiments conducted under the same initial conditions (flow rate $Q = 0.004$ ml/min, alcohol concentration $C = 9.6\%$, bubble position $x = 1.1$ cm) but for different bubble sizes. The bubble size was determined by the ratio of the vertical bubble size to the vertical channel size, $s = h_b/h$. Figure 5a shows the interferograms and corresponding two-dimensional OPD fields obtained for different bubble sizes. Figure 5b presents the corresponding dependencies characterizing the variation of the initial concentration difference ΔC along the channel. Additionally, for comparison, the dependency obtained in an experiment conducted under the same flow rate but in the condition of pure diffusive mixing (in the absence of a bubble) is also presented.

The shaded area on the graph (Figure 5b) represents the region where the bubble position was masked during processing. We did not perform the OPD calculation for this region. It is evident that at the beginning of the channel, the liquids are weakly mixed due to the diffusion process. Near the bubble, the mixing intensifies due to the activation of the convective mechanism. Analysis revealed that the mixing process enhanced with increasing bubble size. It is explained by the fact that the intensity of soluto-capillary Marangoni convection increases with the expansion of the free surface area.

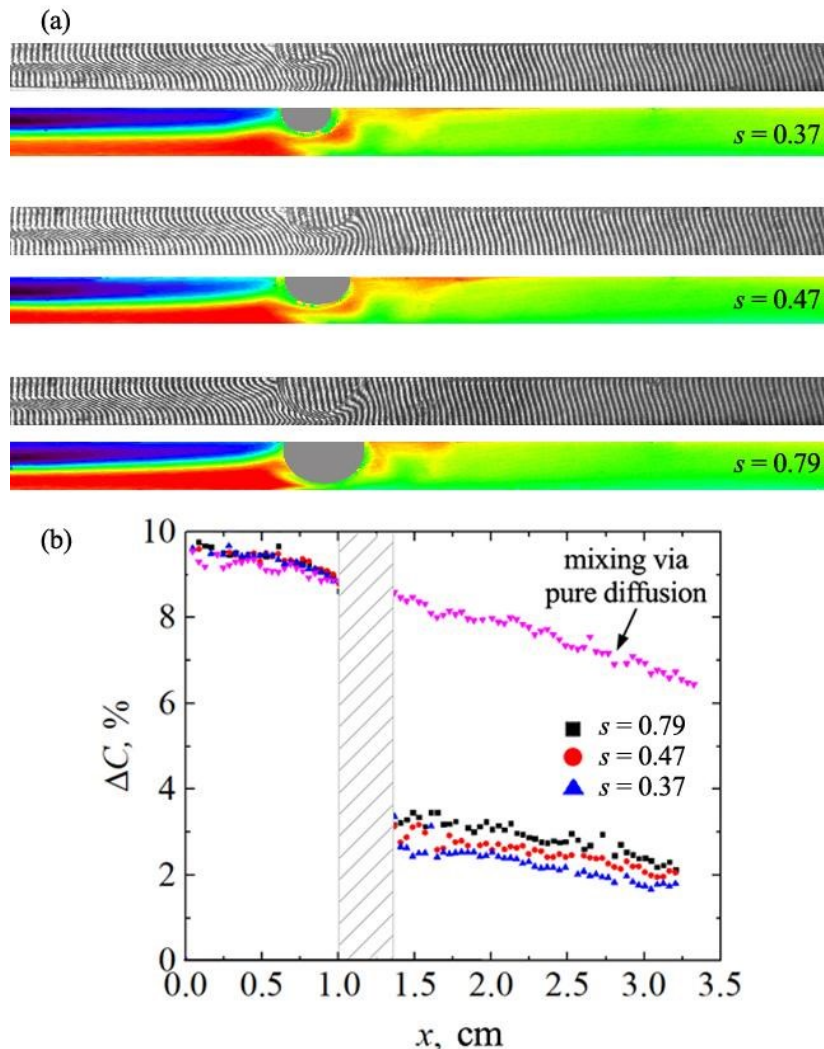


Figure 5. (a) Interferogram (top) showing the mixing process of liquids during the development of Marangoni convection, along with its corresponding OPD field (bottom). Each image has a vertical size of 0.2 cm. (b) Dependencies characterizing the variation of the initial concentration difference between the initial liquids along the channel, obtained for different sizes of gas bubbles. The experimental parameter: flow rate $Q = 0.004$ ml/min, alcohol concentration $C = 9.6\%$, bubble position $x = 1.1$ cm.

4. Conclusion

By employing optical interferometry, we successfully captured and visualized the dynamic mixing process of two continuously flowing liquids within a microreactor, as influenced by two different types of hydrodynamic instabilities. In order to visualize the convective flow driven by the instabilities, we utilized two optical schemes adapted to each specific instability type. The shearing interferometer was employed to reveal the significant inhomogeneities arising from double-diffusion convection. The Fizeau interferometer allowed us to investigate the weaker inhomogeneities associated with soluto-capillary Marangoni convection. The results obtained from our experiments demonstrated the remarkable capabilities of interferometry, even in the context of microreactors with limited spatial dimensions. Despite the challenges posed by confined spaces, the resolution of our experimental apparatus was enough to provide high-quality visualization of the intricate liquid mixing dynamics. The analysis of the interferograms obtained using the Fizeau interferometer yielded qualitative insights and quantitative information about the refractive index distribution within the system. Using the calculated refractive index fields, we derived dependencies that accurately described the variation in the initial concentration difference along the channel. This quantitative assessment enabled us to evaluate the efficiency of the mixing process under different initial system configurations, with varying sizes of the free surface (a gas bubble). This study effectively demonstrates the prowess of interferometry as a powerful tool for both visualizing and analyzing convective flows within microchannels. Our findings have significant implications for the optimization of microreactors and other microdevices, particularly in the context of achieving efficient liquid mixing.

5. Acknowledgments

The work was financially supported by the Russian Science Foundation (grant 19-11-00133).

References

1. Reschetilowski W. *Microreactors in preparative chemistry: practical aspects in bioprocessing, nanotechnology, catalysis and more*. Weinheim, Germany: John Wiley & Sons, 2013. 352 p.
2. Jensen K.F. Microreaction engineering – is small better? // *Chem. Eng. Sci.* 2001. Vol. 56. P. 293-303. DOI: 10.1016/S0009-2509(00)00230-X
3. Hessel V. L., Holger-Schönfeld F. Micromixers – a review on passive and active mixing principles // *Chem. Eng. Sci.* 2005. Vol. 60. P. 2479-2501. DOI: 10.1016/j.ces.2004.11.033
4. Minakov A., Rudyak V., Dekterev A., Gavrilov A. Investigation of slip boundary conditions in the T-shaped microchannel // *Int. J. of Heat and Fluid Flow.* 2013. Vol. 43. P. 161169. DOI: 10.1016/j.ijheatfluidflow.2013.04.002
5. Cai G., Xue L., Zhang H., Lin J. A review on micromixers // *Micromachines.* 2017. Vol. 8. No. 9. P. 274. DOI: 10.3390/mi8090274
6. Lobasov A. S., Minakov A. V., Rudyak V. Y. Study of the mixing regimes of a fluid and a nanofluid in a T-shaped micromixer // *Journal of Engineering Physics and Thermophysics.* 2018. Vol. 91. P. 124-135. DOI: 10.1007/s10891-018-1726-y
7. Tian Y., Chen X., Zhang S. Numerical Study on Bilateral Koch Fractal Baffles Micro-mixer // *Microgravity Sci. Technol.* 2019. Vol. 31. P. 833-843. DOI: 10.1007/s12217-019-09713-x
8. Siraev R., Ilyushin P., Bratsun D. Mixing control in a continuous-flow microreactor using electro-osmotic flow // *Math. Model. Nat. Phenom.* 2021. Vol. 16. P. 49. DOI: 10.1051/mmnp/2021043
9. Bratsun D., Siraev R., Pismen L., Mosheva E., Shmyrov A., Mizev A. Mixing Enhancement By Gravity-dependent Convection in a Y-shaped Continuous-flow Microreactor // *Mi-*

Microgravity Science and Technology. 2022. Vol. 34. No. 5. P. 90. DOI: 10.1007/s12217-022-09994-9

10. Almarcha C., Trevelyan P.M.J., Riolfo L.A., Zalts A., El Hasi C., D'Onofrio A., De Wit A. Active role of a color indicator in buoyancy-driven instabilities of chemical fronts // *The Journal of Physical Chemistry Letters*. 2010. Vol. 1. No. 4. P. 752-757. DOI: 10.1021/jz900418d

11. Dalziel S. B., Hughes G. O., Sutherland B. R. Whole-field density measurements by 'synthetic schlieren' // *Experiments in fluids*. 2000. Vol. 28. No. 4. P. 322-335. DOI: 10.1007/s003480050391

12. Mialdun A., Shevtsova V. Digital Interferometry as a Powerful Tool to Study the Thermodiffusion Effect. // *Comptes Rendus Mecanique*. 2011. Vol. 339. P. 362-368. DOI: 10.1016/j.crme.2011.04.001

13. Malacara D. *Optical shop testing*. John Wiley & Sons, 2007. Vol. 59. 863 pp. DOI:10.1002/9780470135976

14. Huppert H. E., Turner J. S. Double-diffusive convection // *Journal of Fluid Mechanics*. 1981. Vol. 106. P. 299-329. DOI: 10.1017/S0022112081001614

15. Kostarev K., Shmyrov A., Zuev A., Viviani A. Convective and diffusive surfactant transfer in multiphase liquid systems // *Experiments in fluids*. 2011. Vol. 51. P. 457-470. DOI: 10.1007/s00348-011-1063-9

16. Servin M., Cuevas F. J. A novel technique for spatial phase-shifting interferometry // *Journal of Modern Optics*. 1995. Vol. 42. No. 9. P. 1853-1862. DOI: 10.1080/09500349514551621